RNA-Seq Reveals Acute Manganese Exposure Increases Endoplasmic Reticulum Related and Lipocalin mRNAs in *Caenorhabditis elegans*

Martina Rudgalvyte,[1] *Juhani Peltonen,*[1] *Merja Lakso,*[1] *Richard Nass,*[2] *and Garry Wong*[1,3]

[1]A. I. Virtanen Institute for Molecular Sciences, Department of Neurobiology, University of Eastern Finland, Kuopio 70211, Finland; E-mail: *GarryGWong@umac.mo*

[2]Department of Pharmacology and Toxicology, Indiana University School of Medicine, Indianapolis, IN 46202, USA

[3]Faculty of Health Sciences, University of Macau, Avenida da Universidade, Taipa, Macau S.A.R., 999078, China

Received 14 August 2015; accepted 27 August 2015

ABSTRACT: Manganese (Mn) is an essential nutrient; nonetheless, excessive amounts can accumulate in brain tissues causing manganism, a severe neurological condition. Previous studies have suggested oxidative stress, mitochondria dysfunction, and impaired metabolism pathways as routes for Mn toxicity. Here, we used the nematode *Caenorhabditis elegans* to analyze gene expression changes after acute Mn exposure using RNA-Seq. L1 stage animals were exposed to 50 mM $MnCl_2$ for 30 min and analyzed at L4. We identified 746 up- and 1828 downregulated genes (FDR corrected $p < 0.05$; two-fold change) that included endoplasmic reticulum related *abu* and *fkb* family genes, as well as six of seven lipocalin-related (*lpr*) family members. These were also verified by qRT-PCR. RNA interference of *lpr-5* showed a dramatic increase in whole body vulnerability to Mn exposure. Our studies demonstrate that Mn exposure alters gene transcriptional levels in different cell stress pathways that may ultimately contribute to its toxic effects. © 2015 The Authors Journal of Biochemical and Molecular Toxicology Published Wiley Periodicals, Inc. J. Biochem. Mol. Toxicol. 30:97–105, 2016; View this article online at wileyonlinelibrary.com. DOI 10.1002/jbt.21768

KEYWORDS: **Transcriptomics; Heavy Metal; Model Organism; Next-Generation Sequencing; RNAi**

Correspondence to: Garry Wong.

Supporting Information is available in the online issue at www.wileyonlinelibrary.com.

INTRODUCTION

Manganese (Mn) is an essential nutrient that takes part in biological reactions, plays a role in metabolism, and is required as a cofactor in a variety of enzymes. Exposure to Mn occurs most commonly via oral dietary administration or inhalation during occupational activities. Overexposure to Mn, however, may cause a neurological disorder termed manganism. Inhaled Mn can enter the blood–brain barrier and reach the central nervous system accumulating in the brain [1, 2]. As a result of neurological impairment, individuals overexposed to Mn experience weight loss, altered behavior, and decreased fertility [3, 4].

Studies in rodents [3, 5–7], nematodes [8, 9], cell cultures [10], and humans [2] have shown manganese to be neurotoxic. Mn causes apoptotic cell death, and both endoplasmic reticulum (ER) stress and mitochondria function have been implicated as mediator pathways [7, 11]. Within the ER, misfolded or unfolded proteins activate the unfolded protein response (UPR) [12, 13], whereas prolonged UPR may induce apoptosis [14]. Mn can accumulate in mitochondria [5], increase reactive oxygen species and glutathione production, disrupt mitochondria membrane potential [8, 15, 16], increase mitochondria permeability, and inhibit ATP-production [16]. Mn-induced oxidative stress and mitochondrial dysfunction can cause mtDNA single-strand breaks [6] and can also lead to disruption of neurotransmitter release and apoptotic neuron death [17].

RNA-Seq is a recently developed global transcriptomic approach to identify genes that are present, their abundance levels, and their dynamic fluctuations during development, aging, and pharmacological and toxicological conditions [18]. As an approach in

next-generation sequencing technologies, RNA-Seq can provide highly sensitive and specific data regarding the levels of RNA transcripts from biological samples that may reflect eventual protein levels. It has also been used in a variety of model systems to gain insight into toxicologic processes of heavy metals such as copper, methylmercury, and lead [19–21].

While the individual molecular pathways mediating Mn toxicity are being teased apart, the effects of Mn at a global transcriptomic level are poorly understood. Here, we incorporate RNA-Seq to identify the gene expression alterations following acute Mn exposure to understand changes effected by acute Mn exposure in a whole animal model. Our results are consistent with prior studies that indicate dysfunctional oxidative stress- and mitochondria-associated pathways play a role in the toxicity but also show endoplasmic reticulum– and lipocalin-related pathways are altered via activated in blocked UPR (*abu)*, FK506-binding protein family (*fkb)*, and lipocalin-related (*lpr)* gene families.

MATERIALS AND METHODS

C. *elegans* Maintenance and Treatment

C. elegans strains wild-type (WT) Bristol N2 and RNAi-sensitive mutant NL2099 (*rrf-3(pk1426)*) were obtained from the Caenorhabditis Genetics Center (St. Paul, MA) and maintained at 20°C temperature on nematode growth media (NGM) plates containing OP-50 bacteria according to standard protocols [22]. Synchronization of the worms was carried out using potassium hypochlorite solution to bleach the gravid adults and washing embryos 4× in M9 buffer afterwards. Embryos were incubated in M9 buffer for 18 h at room temperature to obtain fully synchronized population. L1 larvae were exposed to $MnCl_2$ (50 mM for 30 min) or potassium gluconate (75 mM for 30 min) for an osmotic control. Worms were washed 3× with M9 buffer and placed onto NGM plates seeded with OP-50 bacteria. Animals were allowed to grow at 20°C until reaching L4 stage just before adulthood for RNA isolation. For chronic $MnCl_2$ treatment, minimal agar plates (1.7% agar, 5 μg/mL cholesterol) were used to avoid $MnCl_2$ precipitation.

RNA Isolation and Sequencing

Both control and $MnCl_2$-treated worms were collected from agar plates at L4 stage, washed 4× with sterile water and placed immediately into a Trizol solution (Gibco-BRL, Gaithersburg, MD). Total RNA was isolated according to manufacturer's protocol. Quantification of RNA samples were performed using Nanodrop device (Thermo Scientific, Wilmington, DE). To avoid DNA contamination, samples were treated with the Turbo DNA-free DNAse kit (Ambion, Austin, TX). DNA-free total RNA samples were sequenced using the Illumina library sample kit (Illumina, San Diego, CA). Samples were run in duplicate on the Illumina HiSeq 2500 instrument at the Millard and Muriel Jacobs Genetics and Genomics Laboratory of California Institute of Technology (Pasadena, CA). Sequences were obtained in a single-read 50 mode.

RNA-Seq Analysis

The number of reads obtained from duplicate samples was 30.9M/33.9M and 32.1M/28.4M from the osmotic control and $MnCl_2$-treated samples, respectively. Reads were aligned to the *C. elegans* genome (WS220) using TopHat implementation 2.0.13 of Bowtie 2.2.4.0 [23] using parameters previously described [20]. The percentage of mapped reads exceeded 94.0% for all samples. To identify differential gene expression, analysis was performed using Cuffdiff program of Cufflinks 2.2.1 [23] with false discovery rate–corrected p values (q values) of <0.05 and fold change > 2 or < 0.5. Gene enrichment analysis was performed for up- and down-regulated genes using DAVID Functional Annotation Tool 6.7 [24].

Quantitative Real-Time PCR (qRT-PCR)

Based on RNA-Seq results, 17 genes were selected and regulated expression verified using the qRT-PCR method. Total RNA from $MnCl_2$-treated and osmotic control *C. elegans* were isolated from L4 stage worms as described above. cDNA synthesis was performed using the Revert-Aid kit (Thermo Fisher Scientific, Waltham, MA) according to the manufacturer's instructions using 0.5 μg of total RNA as a template. Gene-specific oligonucleotide primers for qRT-PCR were designed using Primer- BLAST [25] and obtained from Oligomer OY (Helsinki, Finland). The Maxima SYBR green qPCR Master mix (Thermo Fisher Scientific) was used for amplification reactions according to the manufacturer's protocol. Reactions were performed in iCycler 1.0 system (Bio-Rad, Hercules, CA). Four independent biological replicates were used for this analysis. Each of four biological replicates was performed in technical duplicates. Gene expression differences were calculated using delta-deltaCT method [26] normalized to *act-1*. Oligonucleotide sequences for PCR were as follows:*act-1-5*'-TCGGTATGGGACAGAAGGAC; *act-1-3*'-

CATCCCAGTTGGTGACGATA;	*lpr-1-5′-*	TGGTACACAGTTGTTGATTC;	*lpr-1-3′-*
GTATGGAGTTTGAAGTACCA;	*lpr-3-5′-*	TCTTATCGGACTTCTATCTA;	*lpr-3-3′-*
TGGAGAGGGCATCGCTCACT;	*lpr-4-5′-*	CTCCAATTCTGCTGATGCCG;	*lpr-4-3′-*
TCGTATTGCTTGTACTCATT;	*lpr-5-5′-*	ATGTATTTGCAAGAGATACT;	*lpr-5-3′-*
TCATTGACAACTGGTTCGTA;	*lpr-6-5′-*	CAAAGTTGGACCAGGACAAT;	*lpr-6-3′-*
GGTCCAGCTCCGATAATGTA;	*lpr-7-5′-*	ATATGCAGGATGATCCGTGT;	*lpr-7-3′-*
ATACTGGTTGTGTTGCTTAT;	*abu-7-5′-*	GCCAGTCCTCATGTGTCCAG;	*abu-7-3′-*
TTCTGGTTGGTGTTGGTATT;	*abu-9-5′-*	TTCATCACACTCGCTGTATT;	*abu-9-3′-*
TGAACCTGTTGGCAAGAGCA;	*egl-46-5′-*	CATAAAGGAGGAGGCGGATG;	*egl-46-3′-*
GACTCCTCGGTGACCTCTAC;	lad-2-5′-	GACTCGTTGGCGAACTTTAC;	*lad-2-3′-*
TCATCAGGCACATCTTCTCC,	*ham-1-5′-*	ACTTCTTTGGGTGACTTGGG;	*ham-1-3′-*
CGTCTGCCGAACCATTTCAA;	*ant-1.3-′-*	ATGACTGGAGGAGGAGATTC;	*ant-1.3-3′-*
CCTCTGTAGAGTCCGATTGG;	*ant-1.4-5′-*	ATGTCTGGAGGTGGAGATTC;	*ant-1.4-3′-*
AGAAACCTCTGTAGAGTCCG;	*fkb-3-5′-*	AATGACCGTTCATGGACCAC;	*fkb-3-3′-*
GTTGCTTCCAATCACCTTAC;	*fkb-4-5′-*	AGAGCTGGAAGGAAGATGAC;	*fkb-4-3′-*
AGTCGAGTCTTTCGCAAATC;	*fkb-5-5′-*	GAAGCCATACACCTTCACCC;	*fkb-5-3′-*
CCATTCCCTTGATGACTTCATT;	*fkb-7-5′-*	CCATTACAAGGTGTTCACAG;	*fkb-7-3′-*
ATTCCTTTCAGACCCTTATC.			

RNA Interference and Whole Body Vulnerability Assay

RNA-mediated interference (RNAi) was performed on NGM and minimal agar plates containing isopropyl β-D-thiogalactoside (IPTG, 1 mM) and ampicillin (100 μg/mL). Plates were seeded with RNase III-deficient *Escherichia coli* bacteria strain HT115 (DE3), carrying L4440 vector with the gene fragment (*lpr-5*) (GeneService, Source BioScience, PLC, Nottingham, UK) or empty vector (Addgene, Cambridge, MA). Bacteria cultures for the RNAi-feeding plates were grown for 17 h in liquid LB medium with 100 μg/mL ampicillin. IPTG (1 mM) was added, and cultures were grown for 1 h more and spread onto plates. Synchronized L1 stage worms were transferred onto RNAi$_{(lpr\text{-}5)}$ bacteria containing plates to knock down the *lpr-5* gene expression or plates containing empty L4440 vector for a wildtype control and incubated at 20°C for 48 h. L4 animals were transferred onto minimal agar RNAi plates containing $MnCl_2$ (10 mM) and exposed for 24 h. The number of dead worms was counted. Worms were considered dead if a touch on the nose with a wire pick did not cause any movement. At least 50 worms were counted for each experiment and the experiment was repeated three times. Results are presented as an average $\pm$ SD.

RESULTS

RNA-Seq Analysis of Mn-Exposed *C. Elegans*

We observed 2574 genes to be regulated, of which 746 were up- and 1828 were downregulated. Detailed analysis of the data showed that environmental stress responsive genes were modestly regulated. Heat shock protein family members *hsp-16.41* (1.8 fold), *hsp-16.2* (1.7 fold), and *hsp-16.11* (1.5 fold) were slightly upregulated. In contrast to a prior study [27], our data did not show any significant transcriptional changes to mitochondrion-specific chaperones *hsp-6* and *hsp-60* that participate in the mitochondrial UPR [28] or in ER stress–related chaperone *hsp-4*. Furthermore, we could not observe a significant increase in expression of UPR pathways regulators *atf-6*, *ire-1*, or *pek-1*. However, mitochondrion function–related genes *ant-1.3* and *ant-1.4* were found to be downregulated –3.5 fold and –2.5 fold, respectively. A number of cytochrome P450 (CYP) family genes were also observed to be modulated: *cyp-13B1* (two fold), *cyp-34A1* (2.7 fold), and *cyp-31A2* (–4.2 fold). The complete list of the regulated genes can be found in Supplementary Table 1 in the Supporting Information. The biggest fold changes in the downregulated list belong to the COL family (*col-81* (–9.7 fold), *col-129* (–8.7 fold), *col-178* (–8.5 fold)). The genes with the 20 largest fold changes up and down and their FPKM values (fragments per kilobase of exon per million fragments mapped) are presented in Table 1.

qRT-PCR Confirms LPR and ER-Related Genes

Four independent $MnCl_2$-treated and osmotic control samples from L4 animals were used for verification (Figure 1). Seventeen genes were selected from LPR and ER-related gene families FKB and ABU (*abu-7*, *abu-9*). We also performed PCR with neurogenesis and neuron development related genes *egl-46*, *lad-2*, *ham-1*, and mitochondrion function–related genes (data not shown). The LPR (LiPocalin-Related protein) genes selected were *lpr-1*, *lpr-3*, *lpr-4*, *lpr-5*, *lpr-6*, and *lpr-7* from a total of seven family members. FKB (FK506-binding protein) family members were found to be

TABLE 1. Forty (40) Most Regulated Genes in $MnCl_2$-Treated Compared to Potassium Gluconate-Treated Osmotic Control *C. elegans* Revealed by RNA-Seq

UPregulated				*Downregulated*			
Transcript ID	*WormBase Locus ID (If Available)*	*Fold Change $FPKM_{MnCl2}$/ $FPKM_{control}$*	*FDR-Corrected p-Value (q-Value)*	*Transcript ID*	*WormBase Locus ID (If Available)*	*Fold Change $FPKM_{MnCl2}$/ $FPKM_{control}$*	*FDR-Corrected p-Value (q-Value)*
ZK897.1	*unc-31*	7.57	5×10^{-5}	F38A3.1	*col-81*	–9.68	5×10^{-5}
T10B10.1	*col-41*	5.84	2×10^{-4}	F41F3.4	*col-139*	–9.47	5×10^{-5}
ZK899.4	*tba-8*	5.04	2.9×10^{-3}	Y62H9A.6	na	–9.14	2.6×10^{-3}
F33D11.3	*col-54*	4.99	5×10^{-5}	F55B11.2	na	–9.04	1.05×10^{-3}
M01E10.2	*dpy-1*	4.14	5×10^{-5}	Y62H9A.5	na	–8.99	1.9×10^{-3}
F41D3.3	*nhr-265*	3.40	2.7×10^{-3}	D1054.10	na	–8.94	5×10^{-5}
W02B8.3	*mltn-3*	3.34	2×10^{-4}	Y45F10C.4	na	–8.83	8.4×10^{-3}
ZC84.1	na	3.27	7.9×10^{-3}	D1054.11	na	–8.72	5×10^{-5}
C14C6.4	*nhr-155*	3.17	4.5×10^{-4}	M18.1	*col-129*	–8.69	5×10^{-5}
M28.1	*cutl-9*	3.17	2.5×10^{-4}	ZK813.1	na	–8.55	3.7×10^{-3}
C29E4.1	*col-90*	3.16	5×10^{-5}	C34F6.2	*col-178*	–8.50	5×10^{-5}
K02D7.6	*grl-26*	3.12	1.8×10^{-3}	C24F3.6	*col-124*	–8.43	5×10^{-5}
ZC373.7	*col-176*	3.12	5×10^{-5}	ZK1193.1	*col-19*	–8.30	5×10^{-5}
K02E7.1	na	3.11	1.8×10^{-3}	F11G11.11	*col-20*	–8.22	5×10^{-5}
F14D7.7	na	3.06	1.9×10^{-3}	C53B4.5	*col-119*	–8.11	5×10^{-5}
F56G4.1	*oac-34*	3.04	1.7×10^{-3}	F11H8.3	*col-8*	–8.11	5×10^{-5}
F41E6.14	*oac-29*	3.04	5×10^{-5}	C04F6.1	*vit-5*	–8.10	5×10^{-5}
Y48E1B.8	na	3.02	5×10^{-5}	F26F12.1	*col-140*	–8.03	5×10^{-5}
T23F1.5	na	3.02	5×10^{-5}	D1086.11	na	–7.95	5×10^{-5}
K06A4.1	*nas-3*	2.95	1.5×10^{-3}	W03G11.1	*col-181*	–7.85	5×10^{-5}

Twenty (20) most upregulated and twenty (20) most downregulated transcripts are shown in each column.
FPKM values are fragments per kilobase of exon per million fragments mapped.
na: not available.

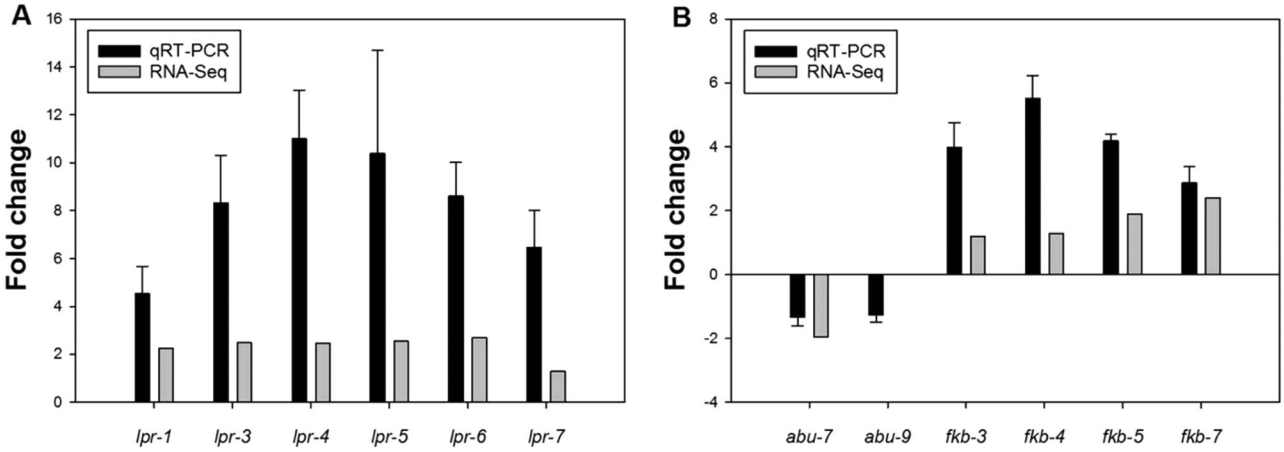

FIGURE 1. qRT-PCR and RNA-Seq analysis of specific genes. Transcriptional changes in LPR family genes (A) and endoplasmic reticulum-related genes (B) observed using RNA-Seq and qRT-PCR were performed as described in Methods. Filled black bars represent qRT-PCR results as the average from four independent samples ± SD. Filled gray bars represent RNA-Seq fold changes for the indicated genes comparing osmotic control (potassium gluconate, 75 mM for 30 min) to $MnCl_2$-treated animals (acute treatment 50 mM for 30 min). Fold changes were calculated using the ΔΔCT method. Negative fold changes were calculated based on –1 treated/control. $p < 0.05$.

regulated including *fkb-3*, *fkb-4*, *fkb-5*, and *fkb-7* from a total of eight family members. The five LPR family members and all four FKB family members were confirmed to be upregulated (more than two-fold change, $p < 0.05$), as well as neurodevelopment-related genes *egl-46* (1.7 fold) and *lad-2* (1.64 fold; data not shown). ABU and ANT (*ant-1.3* (–1.45 fold) and *ant-1.4* (–1.29 fold); data not shown) genes were confirmed to be downregulated. The most highly increased *lpr* gene-based on qRT-PCR results was *lpr-4* (11 fold). The most highly upregulated *fkb* gene was found to be *fkb-4* (5.5 fold).

Functional Annotation and Gene Ontology Enrichment Analysis of Regulated Genes

Gene-set enrichment analysis was performed using a functional annotation tool. Biological themes of genes regulated by $MnCl_2$ were uncovered using DAVID that provided annotation and analysis for statistical enrichment of Gene Ontology (GO) biological processes, cell compartments, and molecular functions (Table 2). Enriched biological processes for upregulated genes were related to positive regulation of multicellular organism growth (31 genes), neuron development (11 genes), neurogenesis (13 genes), and cuticle development (13 genes).

Two hundred seventy-six of the regulated genes were found to belong to cellular compartment integral and/or intrinsic to membrane GO category. Twelve regulated genes were associated with the ER. The most over represented upregulated genes in the ER (Table 2) belong to the FK506-binding protein family (*fkb-3*, *fkb-4*, *fkb-5*, *fkb-7*). The most over represented downregulated genes were genes involved in protein modification (155), meiosis (56), and mitosis (24). A significant amount of genes are also associated with DNA repair (20).

The Lipocalin-Related Protein *lpr-5* Inhibits $MnCl_2$-Induced Animal Death

To determine whether lipocalin-related protein *lpr-5* expression plays a role in Mn-induced toxicity, an RNAi experiment was performed to knock down its mRNA expression. Our study showed that decreased expression of *lpr-5* resulted in increased Mn-induced animal death. After 24 h of Mn exposure, 99% of *lpr-5* knockdown animals were found dead, whereas in the WT group only 27% of the animals were dead. These results suggest that *lpr-5* inhibits Mn-induced animal death (Figure 2).

DISCUSSION

We observed up- and downregulation of two ER-related protein families (FKB, ABU, respectively) that support prior biochemical and cellular studies implicating the ER stress response pathway in Mn toxicity. ABU proteins are related to the apoptosis pathway protein CED-1 that is an integral component of the ER stress pathway that responds to misfolded proteins [29–31]. ABU has previously been shown to be activated when the UPR is blocked genetically or pharmacologically. In our case, ABU gene expression has been found to be downregulated, suggesting UPR impairment. A reason other UPR regulators were not found may be due to protein translocation as

TABLE 2. Enriched GO Biological Process, Molecular Function, and Cellular Compartment Terms among Differentially Expressed Genes in Response to $MnCl_2$ Treatment

Term	*Number of Genes*	*Per Cent*	*p Value*
Enriched biological process for upregulated genes			
Positive regulation of multicellular organism growth	31	4.2	8.4×10^{-5}
Neuron development	11	1.5	3.1×10^{-4}
Neurogenesis	13	1.8	4.2×10^{-4}
Collagen and cuticulin-based cuticle development	13	1.8	5.2×10^{-4}
Neuron projection development	8	1.1	4.9×10^{-3}
Cell morphogenesis involved in neuron differentiation	7	0.9	8.9×10^{-3}
Axonogenesis	7	0.9	8.9×10^{-3}
Proteolysis	35	4.7	1.4×10^{-2}
Enriched biological process for downregulated genes			
Protein modification process	155	8.8	1.6×10^{-33}
Meiosis	56	3.2	6.0×10^{-22}
Mitosis	24	1.4	3.8×10^{-10}
Regulation of cell cycle process	15	0.8	7.8×10^{-7}
DNA repair	20	1.1	2.0×10^{-6}
DNA damage response, signal transduction	7	0.4	4.6×10^{-5}
Regulation of translation	10	0.6	9.5×10^{-5}
Enriched cellular component for upregulated genes			
Endoplasmic reticulum	12	1.6	1.3×10^{-2}
Intrinsic to membrane	276	37.2	1.4×10^{-2}
Cell–cell junction	5	0.7	2.2×10^{-2}
Integral to membrane	274	36.9	2.3×10^{-2}
Enriched cellular component for downregulated genes			
Chromosome	28	1.6	2.4×10^{-9}
Intracellular non-membrane-bounded organelle	73	4.1	2.9×10^{-9}
Cytoskeleton	38	2.1	5.9×10^{-7}
Chromatin	12	0.7	7.9×10^{-4}
Nucleosome	8	0.5	2.8×10^{-3}
Chromosome, centromeric region	5	0.3	1.4×10^{-2}
Nuclear chromosome	4	0.2	4.0×10^{-2}
Enriched molecular function for upregulated genes			
Calcium ion binding	28	3.8	1.9×10^{-7}
Metallopeptidase activity	18	2.4	1.1×10^{-3}
Enriched molecular function for downregulated genes			
Phosphatase activity	84	4.7	3.5×10^{-31}
Protein kinase activity	95	5.4	2.9×10^{-15}
Adenyl ribonucleotide binding	148	8.4	5.2×10^{-12}
Endonuclease activity	9	0.5	1.6×10^{-2}
Double-stranded DNA binding	4	0.2	2.1×10^{-2}

Genes and percent correspond to the number and percentage of the regulated genes that have the GO term annotation indicated.
p Value is a measure of enrichment (Fisher exact test) of the GO term among the genes.

a means of rapid stress response rather than transcriptional change. We also identified four regulated FK506-binding protein (FKB) genes that suggest ER involvement in Mn-induced toxicity. These genes were found to be interacting with *daf-16* and *daf-2* in direct and nondirect pathways [32]. Also, FKB genes were reported to be histone chaperones involved in the regulation of rDNA silencing [33]. This result suggests a potential novel Mn-induced toxicity mechanism.

We also observed mitochondrion-related genes *ant-1.3* and *ant-1.4* to be downregulated by RNA-Seq and confirmed by qRT-PCR (data not shown). It has been hypothesized that *ant-1.3* and *ant-1.4* serve as mediators in mitochondria=generated ATP exchange with cytosolic ADP [34]. Downregulation of these genes suggests energy metabolism impairment. As a result, the mitochondria dysfunction leads to ER stress and UPR, which is consistent with prior reports and this study.

Another finding from the gene list was significant transcriptional changes in the LPR gene family. LPR proteins are low molecular weight lipophilic molecule transporters that participate in intercellular signaling and cellular development. Prior studies have shown that the *lpr-1* protein is required at the time of luminal growth and is expressed in the excretory system, and that null mutants of this gene experience high L1 larvae lethality [35]. Our data reveal *lpr* transcriptional

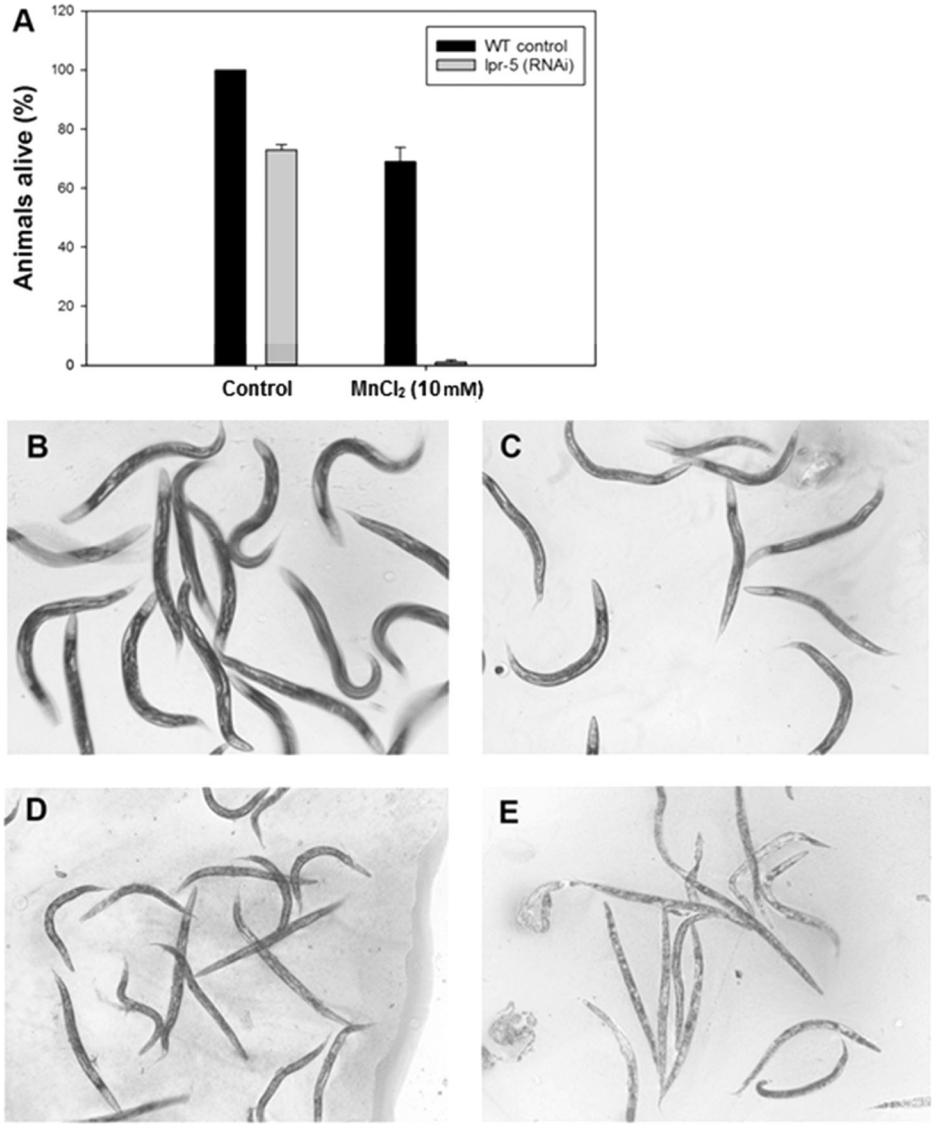

FIGURE 2. Effect of *lpr-5* RNAi on animal lethality caused by Mn. (A) RNAi-sensitive strain NL2099 was grown on plates with the *lpr-5* gene fragment or empty vector (WT control) containing bacteria for 48 h. L4 animals were transferred on $MnCl_2$-containing plates (10 mM) and exposed for 24 h. The number of dead worms was then counted. Results are presented as average ± SD of three independent replicates. *, $p < 0.05$ compared to WT control. (B) WT control worms remained alive and healthy on minimal agar plates. (C) Mn-exposed animals were slightly smaller in size. (D) *lpr-5* (RNAi) knockdown animals developed poorly and were sick. (E) Mn-exposed *lpr-5* (RNAi) knockdown animals were dead.

upregulation caused by Mn exposure, suggesting a new role for the members of this family.

Moreover, *lpr-5* knockdown resulted in an increase in animal death both in nonexposed controls and Mn-exposed samples, suggesting that LPR-5 protein plays an important physiological role at later developmental stages and also in stress conditions. Although the protein function is not clear, LPR-5 provides an intriguing target for future studies to investigate Mn-induced toxicity mechanisms. Interestingly, we also find upregulation of *lpr* family genes and downregulation of *abu* family genes in a previous study of methylmercury exposure [20]. We also found a small number of FKB family members to be regulated by methylmercury (*fkb-4*, 4.6 fold; *fkb-7*, 6.0 fold), although *ant* family genes were not significantly changed [20]. These results suggest that there may be common pathways in heavy metal toxicity.

To our knowledge, this is the first global transcriptome study following Mn exposure in any cell or animal system. Our study highlights transcriptional changes in ER- and mitochondria-associated genes that support current knowledge on the role that these pathways may play in manganism. Furthermore, our study suggests

that genetic pathways involving FKB, CYP, and COL may also contribute to the pathology. Finally, our study provides a unique data resource for investigating Mn and other heavy metal-associated cellular toxicity.

SUPPORTING INFORMATION

Supplementary Table 1. List of up- and down-regulated genes

ACKNOWLEDGMENTS

The authors thank members of the Nass and Wong laboratories for their assistance and discussion of this work. We thank Dr. Igor Antoshechkin for sequencing and Dr. Carina Holmberg-Still for providing the *lpr-5* RNAi clone. Some strains were provided by the *Caenorhabditis* Genetics Center (CGC), which is funded by NIH Office of Research Infrastructure Programs (P40 OD010440). This study was supported in part by the Academy of Finland and grant MYRG2015-00231-FHS from the University of Macau.

REFERENCES

1. Criswell SR, Perimutter J, Huang JL, Golchin N, Flores HP, Hobson A, Aschner M, Erikson KM, Checkoway H, Racette B. Basal ganglia intensity indices and diffusion weighted imaging in manganese-exposed welders. Occup Environ Med 2012;69(6):437–43.
2. Crossgrove J, Zheng W. Manganese toxicity upon overexposure. NMR Biomed 2004;17(8):544–553.
3. Bagga P, Patel AB. Regional cerebral metabolism in mouse under chronic manganese exposure: Implications for manganism. Neurochem Int 2012;60:177–185.
4. Lauwerys R, Roels H, Genet P, Toussaint G, Bouckaert A, De Cooman S. Fertility of male workers exposed to mercury vapor or to manganese dust: a questionnaire study. Am J Ind Med 1985;7(2):171–176.
5. Zhang S, Zhou Z, Fu J. Effect of manganese chloride exposure on liver and brain mitochondria function in rats. Environ Res 2003;93:149–157.
6. Jiao J, Qi Y, Fu J, Zhou Z. Manganese induced single strands breaks of mitochondrial DNA in vitro and in vivo. Environ Toxicol Pharmacol 2008;26:123–127.
7. Quintanar L, Montiel T, Marquez M, Gonzalez A, Massieu L. Calpain activation is involved in acute manganese neurotoxicity in the rat striatum in vivo. Exp Neurol 2012;233:182–192.
8. Settivari R, LeVora J, Nass R. The divalent metal transporter homologues SMF-1/2 mediate dopamine neuron sensitivity in *Caenorhabditis elegans* models of manganism and Parkinson's disease. J Biol Chem 2009;284(51):35758–35768.
9. Vanduyn N, Settivari R, Wong G, Nass R. SKN-1/Nrf2 inhibits dopamine neuron degeneration in a *Caenorhabditis elegans* model of methylmercury toxicity. Toxicol Sci 2010;118(2):613–624.
10. Alaimo A, Gorojod RM, Miglieta EA, Villarreal A, Ramos AJ, Kotler ML. Manganese induced mitochondrial dynamics impairment and apoptotic cell death: A study in human Gli36 cells. Neurosci Lett 2013;554: 76–81.
11. Xu B, Wu SW, Lu CW, Deng Y, Liu W, Wei YG, Yang TY, Xu ZF. Oxidative stress involvement in manganese-induced alpha-synuclein oligomerization in organotypic brain slice cultures. Toxicology 2013;305:71–78.
12. Xu B, Shan M, Wang F, Deng Y, Liu W, Feng S, Yang TY, Xu ZF. Endoplasmic reticulum stress signaling involvement in manganese- induced nerve cell damage in organotypic brain slice cultures. Toxicol Lett 2013;222: 239–246.
13. Wang T, Li X, Yang D, Zhang H, Zhao P, Fu J, Yao B, Zhou Z. ER stress and ER stress- mediated apoptosis are involved in manganese induced neurotoxicity in the rat striatum in vivo. NeuroToxicology 2015;48:109–119.
14. Malhotra JD, Kaufman RJ. Endoplasmic reticulum stress and oxidative stress: a vicious cycle or a double-edged sword. Antioxid Redox Signal 2007;9(12):2277–2293.
15. Zhang S, Fu J, Zhou Z. Changes in the brain mitochondrial proteome of male Sprague–Cawley rats treated with manganese chloride. Toxicol Appl Pharmacol 2005;202:13–17.
16. Racette BA, Aschner M, Guilarte TR, Dydak U, Criswell SR, Zheng W. Pathophysiology of manganese-associated neurotoxicity. NeuroToxicology 2012;33:881–886.
17. Moberly AH, Czarnecki LA, Pottackal J, Rubinstein T, Turkel DJ, Kass MD, McGann JP. Intranasal exposure to manganese disrupts neurotransmitter release from glutamatergic synapses in the central nervous system in vivo. NeuroToxicology 2012;33:996–1004.
18. Wang Z, Gerstein M, Snyder M. RNA-Seq: a revolutionary tool for transcriptomics. Nat Rev Genet 2009;10: 57–63.
19. Castruita M, Casero D, Karpowicz SJ, Kropat J, Vieler A, Hsieh SI, Yan W, Cokus S, Loo JA, Benning C, Pellegrini M, Merchant SS. Systems biology approach in *Chlamydomonas* reveals connections between copper nutrition and multiple metabolic steps. Plant Cell 2011;23:1273–1292.
20. Rudgalvyte M, VanDuyn N, Aarnio V, Heikkinen L, Peltonen J, Lakso M, Nass R, Wong G. Methylmercury exposure increases lipocalin related (lpr) and decreases activated in blocked unfolded protein response (abu) genes and specific miRNAs in *Caenorhabditis elegans*. Toxicol Lett 2013;222:189–196.
21. Wang Y, Xu L, Chen Y, Shen H, Gong Y, Limera C, Liu L. Transcriptome profiling of radish (*Raphanus sativus* L.) root and identification of genes involved in response to lead (Pb) stress with next generation sequencing. PLoS One 2013;8:e66539.
22. Brenner S, The genetics of *Caenorhabditis elegans*. Genetics 1974;77:71–94.
23. Trapnell C, Pachter L, Salzberg SL: TopHat: discovering splice junctions with RNA-seq. Bioinformatics 2009;25:1105–1111.
24. Huang DW, Sherman BT, Lempicki RA. Systematic and integrative analysis of large gene lists using DAVID Bioinformatics Resources. Nat Protoc 2009;4(1):44–57.
25. Ye J, Coulouris G, Zaretskaya I, Cutcutache I, Rozen S, Madden T. Primer-BLAST: a tool to design target-specific primers for polymerase chain reaction. BMC Bioinform 2012;13:134.

26. Livak K, Schmittgen TD: Analysis of relative gene expression data using real-time quantitative PCR and the 2-ΔΔC*t* method. Methods 2001;25:402–408.
27. Angeli S, Barhydt T, Jacobs R, Killilea DW, Lithgow GJ, Andersen J. Manganese disturbs metal and protein homeostasis in *Caenorhabditis elegans*. Metallomics. 2014;6:1816–1823.
28. Yoneda T, Benedetti C, Urano F, Clark SG, Harding HP, Ron D. Compartment-specific perturbation of protein handling activates genes encoding mitochondrial chaperones. J Cell Sci 2004; 117:4055–4066.
29. Shen X, Ellis RE, Lee K, Liu CY, Yang K, Solomon A, Yoshida H, Morimoto R, Kurnit DM, Mori K, Kaufman RJ. Complementary signaling pathways regulate the unfolded protein response and are required for *C. elegans* development. Cell 2001;107(7):893–903.
30. Yoshida M, Honda M, Watanabe C, Satoh M, Yasutake A. Neurobehavioral changes and alteration of gene expression in the brains of metallothionein-I/II null mice exposed to low levels of mercury vapor during postnatal development. J Toxicol Sci 2011;36(5):539–547.
31. Urano F, Calfon M, Yoneda T, Yun C, Kiraly M, Clark SG, Ron D. A survival pathway for Caenorhabditis elegans with a blocked unfolded protein response. J Cell Biol 2002;158(4):639–646.
32. Zhong W, Sternberg PW. Genome-wide prediction of *C. elegans* genetic interactions. Science 2006;311:1481–1484.
33. Kuzuhara T, Horikoshi M. A nuclear FK506-binding protein is a histone chaperone regulating rDNA silencing. Nat Struct Mol Biol 2004;11(3):275–283.
34. Farina F, Alberti A, Breuil N, Bolotin-Fukuhara M, Pinto M, Culetto E. Differential expression pattern of the four mitochondrial adenine nucleotide transporter ant genes and their roles during the development of *Caenorhabditis elegans*. Dev Dyn 2008;237:1668–1681.
35. Stone CE, Hall DH, Sundaram MV. Lipocalin signaling controls unicellular tube development in the *Caenorhabditis elegans* excretory system. Dev Biol 2009;329(2):201–211.